Journal of Alloys and Compounds 488 (2009) 624–627

Contents lists available at ScienceDirect

Journal of Alloys and Compounds

journal homepage: www.elsevier.com/locate/jallcom

Spectroscopic studies of the 1.5 μm ($^4I_{15/2} \rightarrow {}^4I_{13/2}$) emission from polycrystalline ceramic Er:YAG and Er:KPb_2Cl_5

U. Hömmerich[a,*], C. Hanley[a], E. Brown[a], S.B. Trivedi[b], J.M. Zavada[c]

[a] Department of Physics, Hampton University, Hampton, VA 23668, United States
[b] Brimrose Corporation of America, 19 Loveton Circle, Baltimore, MD 21152, United States
[c] Department of Electrical Engineering, North Carolina State University, Raleigh, NC 27695, United States

ARTICLE INFO

Article history:
Received 9 June 2008
Received in revised form 26 June 2008
Accepted 1 September 2008
Available online 8 November 2008

Keywords:
Insulators
Light absorption and reflection
Luminescence

ABSTRACT

The 1.5 μm emission from Er^{3+} ions continues to be of current interest for applications in optical communications and eye-safe solid-state lasers. Recently, significant attention has been focused on the development of 1.5–1.6 μm Er^{3+} solid-state lasers with resonant pumping of the $^4I_{13/2} \leftrightarrow {}^4I_{15/2}$ transition. The motivation for resonantly pumped Er^{3+} lasers lies in the reduced thermal load, which is critical for high power laser application. In this work we present results of the infrared optical properties of polycrystalline ceramic Er:YAG and Er:KPb_2Cl_5 including absorption and emission studies, lifetime measurements, and calculations of 1.5 μm emission cross-sections using the reciprocity and Fuchtbauer–Ladenburg methods.

1. Introduction

The development of solid-state gain media for the ~1.5–1.6 μm region continues to be of significant current interest for applications in optical communications and eye-safe laser applications [1–3]. Significant advances were recently reported in the development of ~1.6 μm Er^{3+} lasers (e.g. Er:YAG), which are resonantly pumped between Stark levels of the $^4I_{15/2} \leftrightarrow {}^4I_{13/2}$ transition [4–10]. The interest in resonantly pumped Er^{3+} lasers has been stimulated by the availability of new long-wavelength pump sources including Er^{3+} fiber lasers and ~1.5 μm diode-laser arrays. In contrast to pumping into the $^4I_{9/2}$ excited state of Er^{3+} at ~980 nm, resonant pumping of the $^4I_{13/2}$ level provides the advantage of a smaller heat load due to a reduced quantum defect.

The development of high quality ceramic $Y_3Al_5O_{12}$ (YAG) doped with trivalent rare earth ions has made an enormous impact on the field of solid-state lasers and is envisioned to replace single-crystal YAG laser rods used in current applications [11–13]. Transparent ceramics offer several important advantages over single crystals including ease of fabrication at reduced cost, higher rare earth homogeneity and concentration, the possibility of multi-layer structures, and fabrication of larger sizes [11–13]. Many studies on ceramic YAG have been concentrated on the material fabrication, characterization, and laser performance of Nd:YAG and Yb:YAG ceramics for ~1 μm laser applications. Only a few studies were reported so far on the spectroscopic properties of Er:YAG ceramics for solid-state laser applications [14–17]. In most cases, the investigated Er:YAG ceramics had a 50 at.% Er^{3+} concentration, which is too high for 1.5 μm eye-safe laser applications [16,17]. The emission quantum efficiency of the 1.5 μm emission was determined to be only ~26.4% for highly doped Er:YAG ceramics, which was attributed to upconversion and cross-relaxation processes [16]. For quasi-three level laser operation of the $^4I_{13/2} \leftrightarrow {}^4I_{15/2}$ transition it is important to keep the Er^{3+} concentration low (1 at.% or less) in order to minimize re-absorption losses at the laser wavelength and to reduce upconversion losses that depopulate the pump and upper laser levels [1–10].

Compared to oxide and fluoride laser hosts, Er-doped crystals with small maximum phonon energies provide the advantage of reduced non-radiative relaxation rates leading to high emission quantum efficiencies. Ternary lead halides such as KPb_2Cl_5 and KPb_2Br_5 were recently identified as a novel class of low-phonon energy laser hosts [18–26]. Efficient emission at near and mid-IR wavelengths have been reported from several rare earth-doped KPb_2Cl_5 and KPb_2Br_5 crystals [18–24]. Moreover, several laser demonstrations from rare earth-doped KPb_2Cl_5 crystals have been reported including Er:KPb_2Cl_5 (Er:KPC) at 1.7 μm and 4.5 μm [22]. Recently, it was also shown that energy-transfer upconversion processes in Er:KPC are orders of magnitude lower compared to common oxide and fluoride laser hosts, which further reduces heat loading in resonantly pumped 1.5 μm Er^{3+} lasers [23].

* Corresponding author.
E-mail address: uwe.hommerich@hamptonu.edu (U. Hömmerich).

0925-8388/$ – see front matter © 2008 Elsevier B.V. All rights reserved.
doi:10.1016/j.jallcom.2008.09.043

In this paper we report spectroscopic results of the 1.5 μm absorption and emission properties in polycrystalline Er:YAG and Er:KPC. A commercial Er:YAG ceramic was used in these studies, whereas Er:KPC crystals were grown using in-house facilities. The emission cross-sections were determined for low concentration samples (~0.5 at.%) using a combination of the reciprocity and Fuchtbauer–Ladenburg (FL) methods.

2. Experimental considerations

A sample of a polycrystalline ceramic Er:YAG was purchased from Baikowski International Corporation (Charlotte, North Carolina) with the dimension 5 mm × 5 mm × 3 mm. The Er concentration as provided by the manufacturer was 0.5 at.%. The investigated Er:KPC crystals were grown using in-house crystal growth facilities as described previously [21,24]. The synthesized KPC material was purified through a combination of directional solidification, zone-refinement, and chlorination of the melt using research grade HCl gas. The Er:KPC crystals were subsequently grown using a modified Bridgman growth technique.

Absorption spectra were measured using a Cary 5000 spectrophotometer with a fixed spectral bandwidth of 0.5 nm. The near-IR emission was excited using a modulated (70 Hz) 972 nm diode-laser and dispersed with a 0.5-m spectrometer. The spectrometer was equipped with a 600 grooves/mm reflecting grating blazed at 1 μm. The spectral resolution in all emission measurements was ~0.5 nm. A long pass filter with a cut-on wavelength of 1100 nm was placed in front of the entrance slit of the spectrometer to block laser scattering. The emission signal was recorded using a thermoelectrically cooled InGaAs detector in conjunction with a lockin amplifier. All recorded emission spectra were carefully calibrated for the spectral response of the experimental setup. For emission lifetime studies the 965 nm output of a pulsed (5 ns) Nd:YAG pumped Optical Parameteric Oscillator was employed as the pumped source. The entire emission from the $^4I_{15/2} \rightarrow {}^4I_{13/2}$ transition was monitored using a 1.5 μm bandpass filter placed directly in front of the detector. The decay transients were averaged and recorded using a digital oscilloscope.

3. Optical characterization

3.1. Polycrystalline ceramic Er:YAG

The room-temperature absorption spectrum of the $^4I_{13/2} \rightarrow {}^4I_{15/2}$ transition of ceramic Er:YAG is shown in Fig. 1. The spectral position and stark-splittings of the observed absorption lines for ceramic Er:YAG closely matched reported data for single-crystal Er:YAG [1,2,10]. The absorption cross-section was calculated using an Er concentration of 6.9×10^{19} cm^3 as determined by inductively coupled plasma optical emission spectroscopy (ICP-OES). The measured Er concentration agreed well with the nominal concentration of 0.5 at.% provided by the manufacturer.

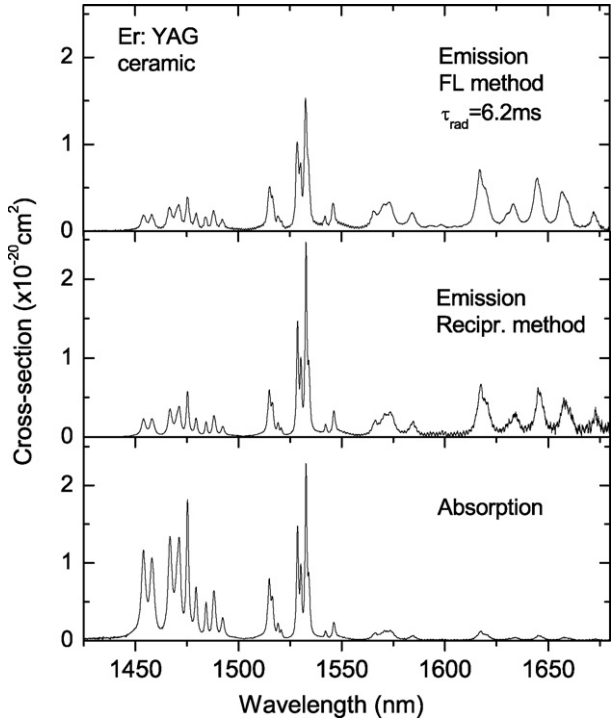

Fig. 1. Absorption and emission cross-section spectra for the $^4I_{15/2} \leftrightarrow {}^4I_{13/2}$ transition of ceramic Er:YAG at room-temperature.

The absorption cross-section for ceramic Er:YAG at the most common pump wavelengths of 1475 nm and 1532 nm were determined to be 1.8×10^{-20} cm^2 and 2.3×10^{-20} cm^2, respectively. At the common Er:YAG laser wavelengths of 1617 nm and 1645 nm, the absorption cross-sections determining ground-state absorption losses were 0.12×10^{-20} cm^2 and 0.06×10^{-20} cm^2, respectively. These numbers are in good agreement with recent spectroscopic results reported for single-crystal Er:YAG (0.5 at.%) [9,10]. It was noticed, however, that the absorption cross-section data reported in the literature vary slightly for single-crystal Er:YAG depending on the Er concentration and spectral resolution employed in the absorption measurements [1–10].

The emission cross-section (σ_{emis}) for ceramic Er:YAG was calculated using the reciprocity method, which relates absorption and emission cross-section [1]:

$$\sigma_{emis}^{recip}(\lambda) = \sigma_{abs}(\lambda)\frac{Z_l}{Z_u}\ \exp\left(\frac{E_{ZL} - hc/\lambda}{kT}\right) \quad (1)$$

where σ_{abs} is the absorption cross-section, Z_l and Z_u are the partition functions of the lower and upper states, and E_{ZL} is the zero-line energy. E_{ZL} is defined as the energy difference between the lowest stark component in the upper and lower levels. The partition function ratio Z_l/Z_u was calculated from published data on the energy level structure of ceramic Er:YAG and yielded a value of 1.055 [17]. The wavelength used for the zero-line (E_{ZL}) was 1526 nm [17]. The obtained emission cross-section spectrum is shown in Fig. 1 and yielded values of 0.67×10^{-20} cm^2 and 0.59×10^{-20} cm^2 at the common laser wavelengths of 1617 nm and 1645 nm, respectively. These cross-sections are similar to reported values for single-crystal Er:YAG [1–10], which further underlines that ceramic Er:YAG has comparable optical properties to its crystalline counterpart. The emission cross-section spectrum was also determined from the well-known FL equation [20]:

$$\sigma_{emis}^{FL}(\lambda) = \frac{\beta\lambda^5 I(\lambda)}{8\pi n^2 c\tau_{rad}\int \lambda I(\lambda)\ d\lambda} \quad (2)$$

where β is the branching ratio, n is the refractive index, c is the speed of light, $I(\lambda)$ is the intensity of the corrected emission spectrum, and τ_{rad} is the radiative lifetime of the $^4I_{13/2}$ multiplet. τ_{rad} was calculated to be 6.2 ms from the condition that the integrated emission cross-sections derived from the reciprocity and FL methods should be equal. The room-temperature lifetime for ceramic Er:YAG powder was measured to be 5.9 ms (see Fig. 2), which supports the internal consistency of the emission cross-section calculations. It was noticed thus, that the measured emission spectrum was slightly impacted by re-absorption losses at wavelengths lower than ~1550 nm, which led to reduced emission cross-sections values compared to those obtained from the reciprocity method. Based on the cross-section analysis, the emission quantum efficiency of the investigated ceramic Er:YAG (0.5 at.%.) sample was estimated to be ~95%, which compares well with the 92.5% emission efficiency reported for single-crystal Er:YAG [10].

3.2. Er:KPb_2Cl_5

The 1.5 μm absorption and emission cross-section spectra ($^4I_{13/2} \rightarrow {}^4I_{15/2}$) for Er:KPC are shown in Fig. 3. In contrast to ceramic Er:YAG, the IR spectra for Er:KPC are relatively broad with only a

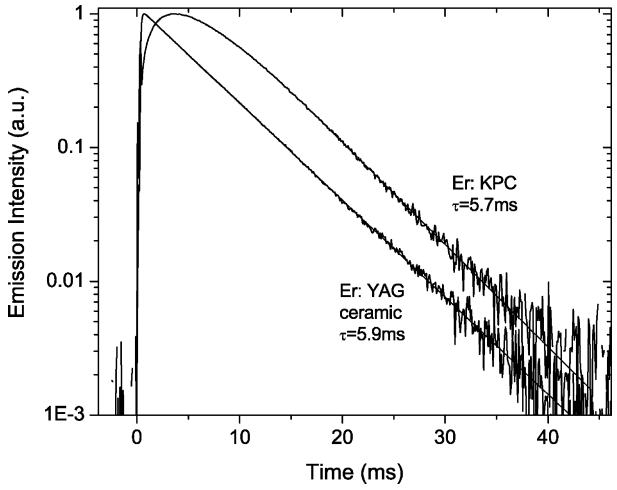

Fig. 2. Emission decay transients for ceramic Er:YAG and Er:KPC excited at 965 nm.

few structures indicating Stark-level splittings. A detailed Stark-level analysis was recently performed on Er:KPC [25,26] indicating a ground-state splitting of ~240 cm^{-1} compared to ~575 cm^{-1} reported for ceramic Er:YAG [17]. The reciprocity method was applied to determine the emission cross-section spectrum for Er:KPC (Fig. 3). The partition functions were calculated from the energy level structure of Er:KPC and the ratio Z_l/Z_u yielded a value of ~1.1 [19,25]. The wavelength used for the zero-line (E_{ZL}) was 1535.4 nm [25]. The resulting peak emission cross-section at 1536 nm was determined to be 1.1×10^{-20} cm^2. The cross-sections at the longer wavelength peaks of 1552 nm and 1582 nm were reduced to values of 0.89×10^{-20} cm^2 and 0.29×10^{-20} cm^2, respectively. For consistency check, the emission cross-section was also calculated using the FL-method as shown in Fig. 3 using a radiative lifetime of 4.3 ms. This lifetime is in good agreement with the radiative lifetime of 4.2 ms derived from a Judd–Ofelt analysis [19].

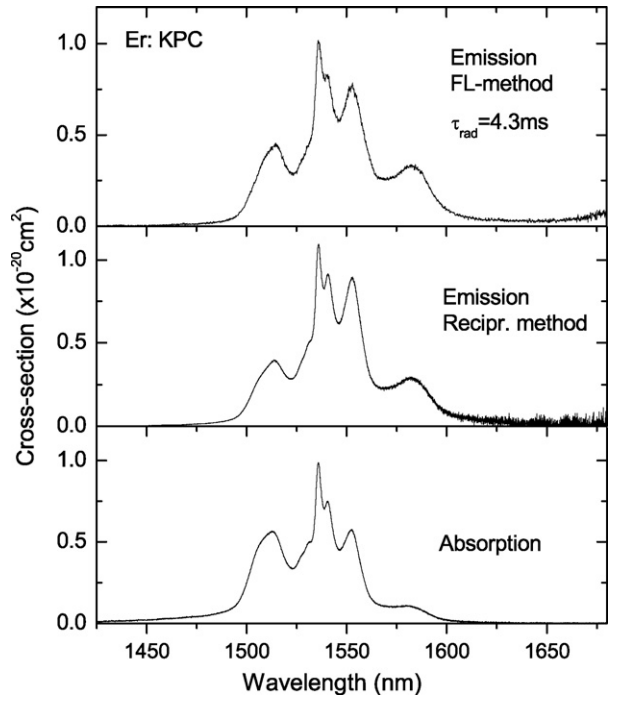

Fig. 3. Absorption and emission cross-section spectra for Er:KPC at room-temperature.

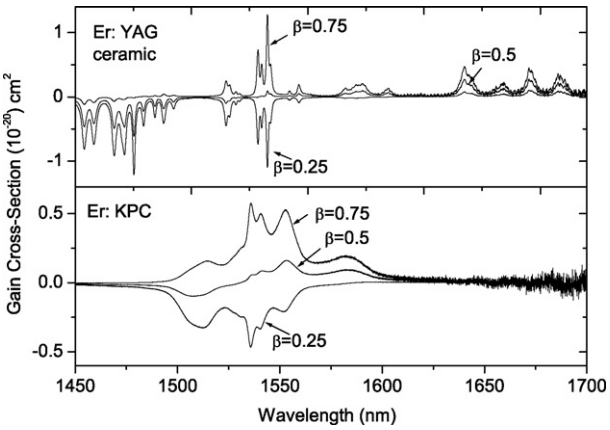

Fig. 4. Gain cross-section spectra for the 1.5 μm transition in ceramic Er:YAG and Er:KPC for different population inversion ratios (β = 0.25, 0.5, and 0.75).

The experimental lifetime from a low concentration Er:KPC powder was determined to be 5.7 ms (Fig. 2), which suggests some residual effect of radiation trapping [19]. The initial rise-time in the 1.5 μm lifetime transient can be attributed to radiative feeding from the $^4I_{11/2}$ excited state.

3.3. Gain cross-sections for ceramic Er:YAG and Er:KPb_2Cl_5

Using the obtained absorption and emission cross-sections for ceramic Er:YAG and Er:KPC the gain cross-sections were calculated according to [2]:

$$g(\lambda) = \beta\sigma_{emis}(\lambda) - (1-\beta)\sigma_{abs}(\lambda) \quad (3)$$

where $\beta = N_{exc}/N_{tot}$ is the inversion ratio with N_{exc} and N_{tot} being the Er^{3+} excited state and total Er^{3+} populations, respectively. Examples of the gain cross-section spectra for β = 0.25, 0.5, and 0.75 are shown in Fig. 4. The peak gain cross-section in Er:KPC for β = 0.75 is only half the value determined for ceramic Er:YAG, which would lead to a significantly higher laser threshold. Furthermore, it can be noticed that higher population inversion ratios are required for Er:KPC than for ceramic Er:YAG to achieve a positive gain cross-section at longer wavelengths. For example, for ceramic Er:YAG already 25% population inversion leads to a gain cross-section of $\sim 0.1 \times 10^{-20}$ cm^2 at the common laser wavelength of 1647 nm. On the contrary, nearly 50% population inversion is needed for Er:KPC to achieve a positive gain of $\sim 0.1 \times 10^{-20}$ cm^2 at the long-wavelength peak at 1582 nm. This can be explained by the larger Stark-level splittings in ceramic Er:YAG compared to Er:KPC, which leads to reduced re-absorption losses at longer wavelengths. However, the significant spectral overlap between the $^4I_{13/2} \rightarrow {}^4I_{15/2}$ emission and $^4I_{13/2} \rightarrow {}^4I_{9/2}$ excited state absorption in Er:YAG leads to a larger energy-transfer upconversion coefficient and higher heat loading compared to Er:KPC [23].

4. Conclusions

Spectroscopic results of the 1.5 μm ($^4I_{15/2} \leftrightarrow {}^4I_{13/2}$) absorption and emission properties of ceramic Er:YAG and Er:KPC were presented. It was observed that the spectral properties and cross-sections of ceramic Er:YAG are very similar to results reported for single crystals of Er:YAG. Therefore, it can be predicted that 1.5–1.6 μm lasers using ceramic Er:YAG will have comparable laser properties to their crystalline counterparts, with the added advantages intrinsic to ceramic gain media. Compared to ceramic Er:YAG, Er:KPC has significantly broader spectral features providing the possibility for modest wavelength tunability in the 1.5 μm region.

The smaller ground-state splitting for Er:KPC compared to Er:YAG, however, leads to significant ground-state re-absorption due to higher thermal populations in the Stark levels of the $^4I_{15/2}$ multiplet. In addition, further improvement in the material purification and crystal growth are necessary to produce laser quality Er:KPC crystals for the 1.5 μm spectral region.

Acknowledgements

The authors at Hampton University acknowledge financial support by the Army Research Office through grant W911NF-04-1-0302 and the National Science Foundation through grants HRD-0630372 and HRD-0734635.

References

[1] S.A. Payne, L.L. Chase, K.K. Smith, W.L. Kway, W.F. Krupke, IEEE J. Quant. Electron. 28 (1992) 2619.
[2] T. Schweitzer, T. Jensen, E. Heumann, G. Huber, Opt. Commun. 118 (1995) 557.
[3] P. Le Boulanger, J.L. Doualan, S. Girad, J. Margerie, R. Moncorge, Phys. Rev. B 60 (1999) 11380.
[4] Y.E. Young, S.D. Seltzer, K.J. Snell, P.A. Budni, T.M. Pollak, E.P. Chicklis, Opt. Lett. 29 (2004) 1075.
[5] S.D. Setzler, M.P. Francis, Y.E. Young, J.R. Konves, E.P. Chicklis, IEEE J. Sel. Topics Quant. Electron. 11 (2005) 645.
[6] D. Garbuzov, I. Kurryashov, M. Dubinskii, Appl. Phys. Lett. 87 (2005) 121101.
[7] D.Y. Shen, J.K. Sahu, W.A. Clarkson, Opt. Lett. 31 (2006) 754.
[8] K. Spariosu, V. Leyva, R.A. Reeder, M. Klotz, IEEE J. Quant. Electron. 42 (2006) 182.
[9] J.O. White, M. Dubinskii, L.D. Merkle, I. Kuryashov, D. Garbuzov, J. Opt. Soc. Am. B 24 (2007) 2454.
[10] M. Eichhorn, S.T. Fredrich-Thornton, E. Heumann, G. Huber, Appl. Phys. B 91 (2008) 249.
[11] A. Ikesue, Y.L. Aung, T. Taira, T. Kamimura, K. Yoshida, G.L. Messing, Annu. Rev. Mater. Res. 36 (2006) 397.
[12] J. Lu, K. Ueda, H. Yagi, T. Yanagitani, Y. Akiyama, A. Kaminskii, J. Alloys Compd. 341 (2002) 220.
[13] J. Dong, A. Shirakawa, K. Ueda, H. Yagi, T. Yanagitani, A.A. Kaminskii, Opt. Lett. 32 (2007) 1890.
[14] M. Sekita, H. Haneda, S. Shirasaki, J. Appl. Phys. 69 (1991) 3709.
[15] G. Qin, J. Lu, J.F. Bisson, Y. Feng, K. Ueda, H. Yagi, T. Yanagitani, Solid State Commun. 132 (2004) 103–106.
[16] D. Sardar, C.C. Russell, J.B. Gruber, T. Allik, J. Appl. Phys. 97 (2005) 123501.
[17] J.B. Gruber, A.S. Nijjar, D.K. Sardar, R.M. Yow, C.C. Russell III, T.H. Allik, B. Zandi, J. Appl. Phys. 97 (2005) 063519.
[18] M.C. Nostrand, R.H. Page, S.A. Payne, L.I. Isaenko, A.P. Yelisseyev, J. Opt. Soc. Am. B 18 (2001) 264.
[19] N.W. Jenkins, S.R. Bowman, S. O'Connor, S.K. Searles, J. Ganem, Opt. Mater. 22 (2003) 311.
[20] K. Rademaker, W.F. Krupke, R.H. Page, S.A. Payne, K. Petermann, G. Huber, L. Isaenko, U.N. Roy, A. Burger, K. Nitsch, J. Opt. Soc. Am. B 21 (2004) 2117.
[21] U. Hömmerich, Ei.Ei. Nyein, S.B. Trivedi, J. Lumin. 113 (2005) 100.
[22] S.R. Bowman, S.K. Searles, N.W. Jenkins, S.B. Qadri, E.F. Skelton, in: C. Marshall (Ed.), Trends in Optics and Photonics, vol. 50, Optical Society of America, 2001.
[23] R.S. Quimby, N.J. Condon, S.P. O'Connor, S. Biswal, S.R. Bowman, Opt. Mater. 30 (2008) 827.
[24] P. Amedzake, E. Brown, U. Hommerich, S.B. Trivedi, J.M. Zavada, J. Cryst. Growth 310 (2008) 2015.
[25] J.B. Gruber, R.M. Yow, A.S. Nijjar, C.C. Russell III, D.K. Sardar, B. Zandi, A. Burger, U.N. Roy, J. Appl. Phys. 100 (2006) 043108.
[26] A. Ferrier, M. Velazquez, J.L. Doualan, R. Moncorge, J. Opt. Soc. Am. B 24 (2007) 2526.